CrossMark

ORIGINAL PAPER

Low-Temperature Carrot Cooking Supported by Pulsed Electric Field—DMA and DETA Thermal Analysis

Jiří Blahovec[1] · **Pavel Kouřím**[1] · **Martin Kindl**[1]

Abstract The paper deals with carrot processing that combines the effect of the electric pulse loading with the low-temperature heating. The pulse procedure was formed by one 10-ms long electric pulse (amplitude, 600 V/cm; basic frequency, 20 kHz) on the 160-ms long electric background less than 30 V/cm. The procedure was followed by the combined dynamic mechanical analysis (DMA) and dielectric thermal analysis (DETA) tests with the initial temperature of 30 °C and final temperature of 90 °C. Humidity in the test chamber was kept at 90 % during the whole heating test, with the heating rate of 1 °C/min. During the whole test, both components of the complex modulus of elasticity (DMA) of the specimen as well as both components of the specimen's permittivity (DETA) were registered. A similar test was also performed with other specimens without the initial pulse procedure. Ratios of corresponding data (storage modulus, loss modulus, dielectric constant, and dielectric loss) are approximately constant up to the temperature of approximately 70 °C where it starts to reduce substantially. The obtained results denote that can be processed using electric pulses reaching the similar state as during the tissue heating.

✉ Jiří Blahovec
blahovec@tf.czu.cz

[1] Department of Physics, Czech University of Life Sciences, 16521 Prague 6-Suchdol, Czech Republic

Abbreviations

A	lower part of temperature scale (in our case cca 30–71 °C)
B	higher part of the temperature range (in our case cca 71–90 °C)
B1	lower part of B (in our case approximately 71–80 °C)
B2	higher part of B (in our case approximately 80–90 °C)
CV (%)	coefficient of variations
DETA	dielectric thermal analysis
DL (−) or (%)	dielectric loss (imaginary part of relative permittivity)
DMA	dynamic mechanical analysis
DP (−) or (%)	dielectric constant (real part of relative permittivity)
E (V/cm)	maximal intensity of the pulse electric field
E_0 (V/cm)	intensity of electric field—parameter of Eq. (2)
IQR	interquartile range Q3–Q1
K (cm/V)	intensity of specimen impedance to pulse field (Eq. (2))
LM (Pa) or (%)	loss modulus
MV	mean value
Q1	first quartile
Q2	second quartile
R (−)	ratio of Z_x and Z_i
SM (Pa) or (%)	storage modulus
SE	standard error
SD	standard deviation
T (°C)	temperature
tg (−)	symbol for loss tangent (in both DEA and DETA)
X_t (Ω)	value of Z_x at infinite E

Z (Ω)	disintegration parameter (Eq. (1), De Vito et al., 2008)
Z_i (Ω)	specimen impedance before pulse
Z_x (Ω)	specimen impedance after pulse
σ (Ω^{-1} m^{-1})	specimen's electric conductivity
σ_d (Ω^{-1} m^{-1})	electric conductivity in disintegrated specimen
σ_u (Ω^{-1} m^{-1})	specimen's electric conductivity before pulse

Introduction

Cooking or cookery is the process of preparing food for consumption with the use of heat (Wikipedia 2015, term "Cooking"). The aim of the cooking is to improve sensory quality of cooked products mainly by adapting of their texture to such a state that is savoury to a consumer. This result can be reached by a combination and or superposition of the traditional heating, thermal effects of electric current and microwaves (Vollmer, 2004), and newly by application of the electric pulses. The external pulsing electric fields (Tsong and Su, 1999, De Vito et al., 2008, Vorobiev and Lebovka, 2010) are also able to damage integrity of the cellular membranes. De Vito et al. (2008) evaluated the state of cellular membranes after combined thermal and pulse electric processing by a special parameter Z (Lebovka et al., 2002), termed disintegration parameter. This parameter is given by the actual value of the material's electric conductivity σ. Z moves between 0 for material in the initial untreated state with conductivity σ_u and 1 for materials with totally disintegrated cellular membranes with conductivity σ_d:

$$Z = \frac{\sigma - \sigma_u}{\sigma_d - \sigma_u} \tag{1}$$

In practical cases, σ_d was estimated by direct conductivity measurement after a long and high electric pulse processing of the tested material (De Vito et al. (2008) used 0.1-s long pulses of intensity 1 kV/cm for apples). The disintegration effect of a process is determined by parameters of the pulse procedure, by temperature of thermal processing and also by time schedule of the whole process (Vorobiev and Lebovka, 2008).

The important role of temperature as an external parameter for living matter is generally known. Even if the knowledge of partial processes caused by temperature variation is relatively good (Garret and Grisham 2010, Gómez et al., 2004), there is still a lack of information about details of the processes taking part in living cells and tissues during their heating. Similarly as in the tissues, the behaviour of cellular complexes has to be studied by indirect methods, in which the characteristic states are indicated. For such purposes, the methods of thermal analysis (Haines, 2002) are used, provided that specimens' drying due to increasing temperature is prevented or at least reduced (Blahovec et al., 2012, Blahovec and Lahodová, 2012b).

Previous success of dynamic mechanical analysis (DMA) in studies of thermally controlled changes in potato tuber (Blahovec and Lahodová, 2012b, Ando et al., 2014) was an inspiration for applying the DMA to carrot (Blahovec and Lahodová, 2012a, Xu and Li, 2014). Whereas in potatoes the main thermal effects were caused by starch transformations, the main thermal effects in carrot were caused by changes in the cellular membranes related to the membrane's proteins denaturation.

The superposition of electric pulses and simple heating procedures could form a new way in the culinary area and the cooking technology. Every reduction of heating in any food processing is a source of reductions in energy consumption (Vollmer, 2004) as well as a source of reduction of food component losses that are caused primarily by application of higher temperatures (Lešková et al., 2006). This is important mainly in fruits and vegetables where heating is followed by losses of vitamins and further unstable important nutrients (De Roeck et al., 2010, Lešková et al., 2006).

Carrot is a good model material for other vegetables; it can serve as a testing medium for detection of changes caused in vegetables by different modifications of food and/or cooking technologies (Hiranvarachat et al. 2011, Lemmens, et al., 2009, Xu and Li, 2014, Georget et al., 2002) and also by application of electric fields (i.e. Leong and Oey, 2014) or application of high pressures (Park et al., 2013, De Roeck et al., 2010). Carrot belongs to vegetables for which the pulse electric fields are of high interest (Lebovka et al., 2002).

In this paper, we use thermal analysis (DMA—dynamic mechanical analysis and DETA—dielectric thermal analysis (Haines, 2002)) for the study of the changes caused in carrot by electric pulses. The aim of this paper is to find a temperature range suitable for the combination of pulse electric and thermal methods in cooking of carrot.

Materials and Methods

Test Material

The carrot (*Daucus carota*, *subsp. sativa*, cv. Jereda) was cultivated in the university farm. The harvested (August 2014), selected, and damage free roots (diameter about 4 cm and length about 15 cm) were washed and shortly stored in plastic bags in a refrigerator (4 °C, 85 % relative humidity). For adaptation to room conditions (temperature and humidity), the roots selected for experiments were left at room temperature on the table and tested the next day.

Specimens

Rectangular specimens measuring 3.8 (width)×5.5 (thickness)×35 (length)mm with the long axis parallel to the root

axis were cut from the myzoderma (outer part of the tested roots) using special cutting jigs. From one root, four specimens were prepared. Part of the specimens was treated with a special pulsing test prior application of the thermal analysis; the other part of the specimens was used for thermal analysis without pulse processing. Complex impedance of specimens was measured between two electrodes in a special fixing jig (Fig. 1b, fixing jig) where the specimen's cross section is formed by its width multiplied by a part of its length (20 mm) and the distance between electrodes is formed by the specimen's thickness.

Pulse Loading

Pulse loadings were performed using a special equipment constructed for this purpose (for more details, see Šmejkal et al. 2011). Block scheme of the equipment is given in Fig. 1a and its photo in Fig. 1b. The basic sinusoidal AC signal with a frequency of 20 kHz was produced by a waveform generator (in Fig. 1b denoted as generator). The obtained signal was modulated to have a form of one approximately rectangular alternated pulse (mean pulse amplitude termed as the pulse height is the basic parameter, length 10 ms). The length of the whole process was 160 ms; the field level outside the pulse was below 30 V/cm. The process was directed by a programmable microprocessor. The signal was amplified by an acoustic amplifier (Fig. 1b), and the whole process was directed by a computer using the programme means of LabView 2009 (National Instruments). The described procedure was motivated partly by limitations of the used instruments and also by our aim to minimize heating of the tested specimen during the pulse procedure.

The final signal was transformed to desired level and conducted to electrodes in the fixing jig. The electric contacts between conductors and specimen were improved by weights about 0.1 kg. Typical voltage and current forms of the pulse are given in Fig. 1c. From the figure, it is clear that the pulses are not fully rectangular; in the evaluation of our results we, used mean values of the pulse amplitudes. The changes of specimen properties were detected by the impedance measurements, prior and post the pulse procedure (by an RLC meter—see Fig. 1b).

DMA Analysis

The DMA experiment was performed with a special DMA instrument, constructed by RMI Company (Pardubice, Czech Republic), model DX04TC with a single cantilever fixing of specimens. The specimen was carefully mechanically fixed in two points (more details on fixing was given by
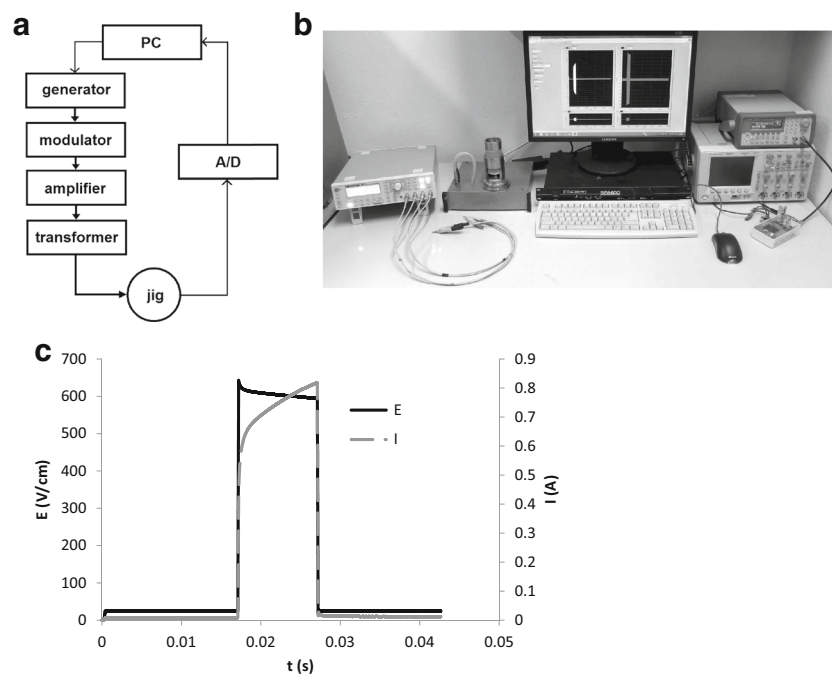

Fig. 1 Pulse loading of the carrot specimens. **a** Block scheme of the equipment: *A/D* A/D converter, *PC* computer. **b** Photo of the equipment; from the *right side*—pulse generator of rectangular pulses (generator Agilent 33220A) with oscilloscope (Agilent DSO6014A), acoustic amplifier Mc Crypt SPA 600 with computer monitor and computer keyboard, box with electronic circuits inside and fixing jig (the jig was also used for fixing the specimens during DMA/DETA test), and RLC meter Hameg 8118; **c** Profile of the electric pulse that is used for pulsing the carrot specimens; *E* denotes electric field intensity and *I* electric current; the *curves* denote amplitudes of the alternate signals of frequency 20 kHz

Kindl, 2014) so that the longitudinal axis was perpendicular to the fixing jaws. The free length of the specimen between the jaws was 10.8 mm. The height of the fixed specimen was approximately 3.8 mm. One of the jaws was fixed and the other moved up and down with a constant amplitude of 1 mm and a frequency of 1 Hz. The force connected with the oscillation was recorded, being the basis for the complex modulus determination. Every experiment started at a temperature of 30 °C; the real part of the complex modulus of elasticity (denoted as the storage modulus—SM) was denoted as 100 % at this temperature and further values of both components were recalculated under this value. The imaginary part of the modulus of elasticity was denoted as the loss modulus (LS) in agreement with previous papers (e.g. Blahovec et al., 2012). Alternatively, the measured module values were expressed in ordinary physical units (i.e. Pa). Air humidity in the test chamber was 90 % and was kept constant during the whole experiment. The control of air humidity in the test chamber was based on direct humidity measurement by a special hygrometer as the basis for water vapour ejection into the chamber. The humidity control system was supplied as a part of the DMA model DX04TC. The temperature scan proceeded up to 90 °C with the rate of 1 °C/min.

DETA Analysis

The DMA instrument was arranged for parallel measurement of the electric properties of the tested specimen either as a real conductor (described by the complex impedance) or a real capacitor (described by the complex permittivity); for details, see Kindl (2014). The wave generator Agilent 33522A working at a frequency of 10 kHz and voltage of 1 V was used as a source in a serial circuit with the specimen and the standard resistor 2.21 kΩ. Effective voltages on source, specimen, and the standard resistor were measured continually, and the obtained values were used to calculate both real and imaginary values either of the specimen's impedance or its permittivity (for details, see Kindl, 2014). Similarly as in the DMA part, the obtained complex values were expressed either by their physical values (the relative permittivity by the dimensionless numbers and the impedance in Ω) or in percent of the values measured at 30 °C (for the permittivity, it was its imaginary part, and the impedance was based on its real part). The real part of relative permittivity was termed also as the dielectric constant (DP) and the imaginary part of the relative permittivity was denoted also as the dielectric loss factor (DL), and their ratio DL/DP expressed the loss tangent.

Data Analysis

The obtained results were analysed using the standard laboratory software Origin®, OriginPro Ver. 7 (OriginLab, Northampton, MA, USA). Measured data were smoothed by averaging of 5 adjacent points followed by differentiating the smoothed data. The obtained data were classified and unified into 1 °C wide classes. The outliers were identified by Tukey outlier filter (Hoaglin et al., 1983) and filtered from data sets. $Y < (Q1 - 1.5 IQR)$ and $Y > (Q3 - 1.5 IQR)$, where Q1 and Q3 were the first and third quartiles, respectively, and Y represents the outlier. The interquartile range was calculated as follows: IQR=(Q3-Q1).

Results and Discussion

Determination of the Pulse Level

The initial impedance of the tested specimens was 1761 and 1326 Ω for the real part and imaginary one, respectively, with coefficients of variation of 16 and 14 %, respectively ($n=70$). Change of both components after pulses is given in Fig. 2, where the ratio of the resulting value (after 5 s and after 120 s) and the initial value prior pulsing is plotted. The measured values of impedance after pulses Z_x could be described as a
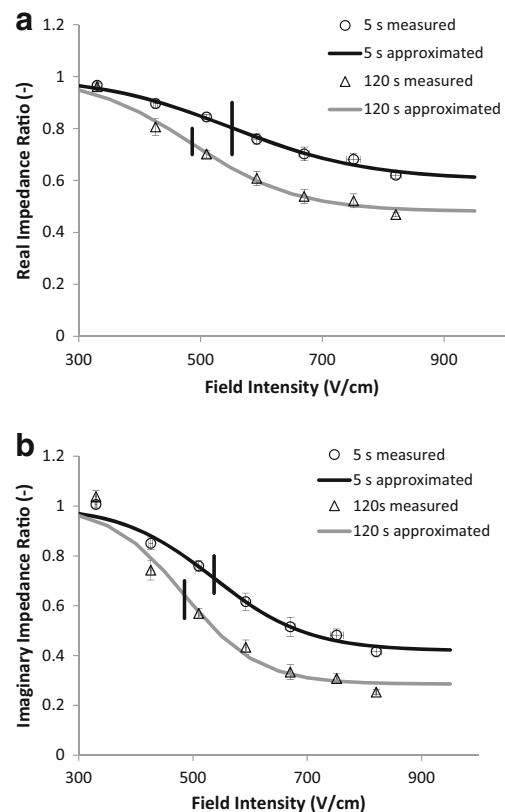

Fig. 2 Relative specimen impedance plotted against electric field intensity in double pulse loading. The measured values are approximated by the modified Fermi's equation—Eq. (2). *5 s* denotes measurement just after the pulsing (5 seconds), *120 s* denotes measurements after 2 min after pulsing. *Crossing lines* denote corresponding values of E_0 in Eq. (2). **a** Real part of the impedance. **b** Imaginary part of the impedance

function of the pulse field intensity E by a modified Fermi-like function (e.g. Kittel, 2005):

$$R = \frac{Z_x}{Z_i} = X_t + (1-X_t)\frac{[e^{-kE_0} + 1]}{e^{k(E-E_0)} + 1} \qquad (2)$$

where Z_i is the initial impedance of specimen prior to the pulses (see higher) and X_t, k, and E_0 are parameters. Parameter X_t denotes a relative part of the impedance that was not reduced by the pulses, k is related to sensitivity of impedance to the pulse field, and E_0 is a characteristic Fermi-like parameter, the value of field intensity corresponding little more than one half of the maximal possible decrease. Equation (2) fulfils two important solutions: for the zero E, it gives 1 and for the infinite E, it gives X_t.

The parameters of Eq. (2) are given in Table 1. The obtained values depended on the measured values. For both imaginary parts of impedance and later measured values (after 120 s) of the real part of impedance, the parameters k were higher (i.e. the tissue was more sensitive to the pulse intensity). The values of E_0 and X_t were lower in later measurements and generally lower for the imaginary part than the real one, expressing easier and higher change of impedance in the cases with lower E_0 and X_t values. It denoted nontrivial relations between the internal changes in carrot tissue and the physical mechanisms controlling both components of impedance. Moreover, the impedance aftereffects, i.e. the time dependences of the measured values, indicated the existence of some nonphysical processes in the pulsed tissue (Gómez Galindo et al., 2008).

The obtained values of E_0 close to 500 V/cm indicated that the electric fields of such intensity were high enough to change the internal structure of pulsed specimen so much to be detectable by thermal analysis. This result is in agreement with the results reviewed by Vorobiev and Lebovka (2008). We selected the value 600 V/cm, a little higher than the E_0 values, as a basic value for our experiments. We worked with two kinds of specimens: the initial, without any pulse procedure, and pulsed, with the above-described pulse procedure with pulse field intensity $E=600$ V/cm.

DMA Plots

The temperature scans of the modulus of elasticity are given in Fig. 3. Figure 3 shows a general decrease of elastic modulus with increasing temperature. The module decreases were generally fluent. Some indications of irregularity were detected at temperatures above 50 °C. The observed absolute values cannot be interpreted as the precise ones because of some experimental parameters that are not under control (inexact specimens' cross sections, inexact realization of the bending, etc.). The important part of the DMA test is its reproducibility that makes possible to compare results obtained with pulsed and initial specimens. Figure 3 clearly shows that the data measured at pulsed carrot were lower than the corresponding ones obtained at the carrot that was not pulsed prior to the DMA test.

This difference was quantified by calculating and plotting the ratio between parameters measured at both types of specimens. The obtained results for both module components SM and LM and their ratio LM/SM—it is termed loss tangent— are plotted in Fig. 4. This figure shows that the whole temperature scale can be divided into two parts: the first one, up to the temperature approximately 71.5 °C (A), and the second one, at the higher temperatures (B). In part A, the plotted ratios for SM and LM increased with increasing temperature nearly equidistantly: the slopes of lines used for approximation were 0.0041 and 0.0035 K^{-1}, respectively. Loss tangent ratio was then nearly constant in this part: about 1.2 (more exactly 1.19), indicating that loss tangent of the pulsed specimens was about 20 % higher in part A than the loss tangent of the initial specimen. The pulsed carrot was softer in this part than the initial specimens. In part B, the differences between pulsed and the initial specimens decreased and values of the plotted ratios moved to 1: most clearly, it was given at the loss tangent. We can understand that at temperatures in part B, the changes caused by heating were so high that the effects of the pulses were then hidden and/or overlapped by the effects of the high temperature. The DMA results are in agreement with our previous results

Table 1 Parameters of Eq. (2)

Parameters	5 s				120 s			
	Real		Imaginary		Real		Imaginary	
	MV	SE	MV	SE	MV	SE	MV	SE
k (cm/V)	0.0090	0.0015	0.0122	0.0023	0.0117	0.0019	0.0155	0.0042
E_0 (V/cm)	552	23	537	19	486	15	485	19
X_t (-)	0.602	0.030	0.419	0.037	0.481	0.024	0.286	0.045
R^*	0.760		0.604		0.590		0.389	

*$E=600$ V/cm

E_0 (V/cm), intensity of electric field—parameter of Eq. (2); K (cm/V), intensity of specimen impedance to pulse field (Eq. (2)); MV, mean value; SE, standard error

Fig. 3 Modulus of elasticity of the specimens tested by DMA. *SM* denotes storage (real part) and *LM* loss (imaginary part) of the complex modulus. Term initial means specimens that were not pulsed before the test. *Bars* in the figure denote standard error based on 40 experimental points at least
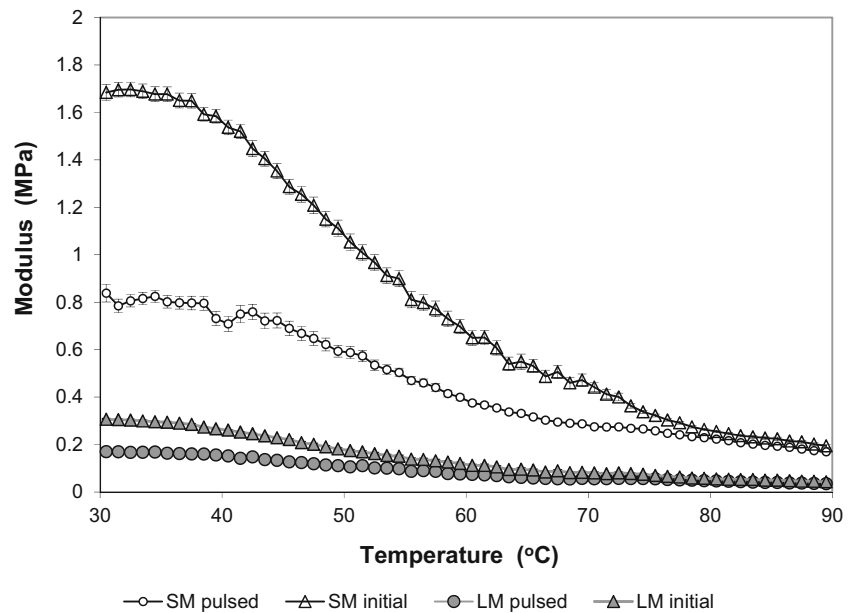
(Blahovec and Lahodová, 2012a) and results of the other authors (Xu and Li, 2014).

DETA Data

The electric data are concentrated in Fig. 5. Figure 5a contains measured values of the dielectric constant (the real part of the relative permittivity), and Fig. 5b contains data for the imaginary part of the relative permittivity (the dielectric losses). Whole data from Fig. 5 indicate also the above-mentioned two temperature ranges: A at temperatures lower than approximately 71.5 °C in which the changes of the parameters with temperature were rather small and B for the higher temperatures at which the parameters strongly changed with

increasing temperature. In the part B at temperatures higher than cca 80 °C, some additional changes of the data can be observed. The main difference between pulsed and initial specimens consists in the higher values of all parameters that were observed in pulsed specimens in comparison to the corresponding data obtained in initial specimens.

Similarly as at the DMA data, the ratios of the pulsed and the initial data were calculated for the DETA test. The results are given in Figs. 6 and 7. In Fig. 6, there are results for permittivity components. The ratios are relatively stable for the dielectric constant (denoted as DP in Fig. 6) at temperatures lower than approximately 70 °C; this value is approximately 1.2. At higher temperatures, in part B, a decrease of this value (B1) and some variation with the further small
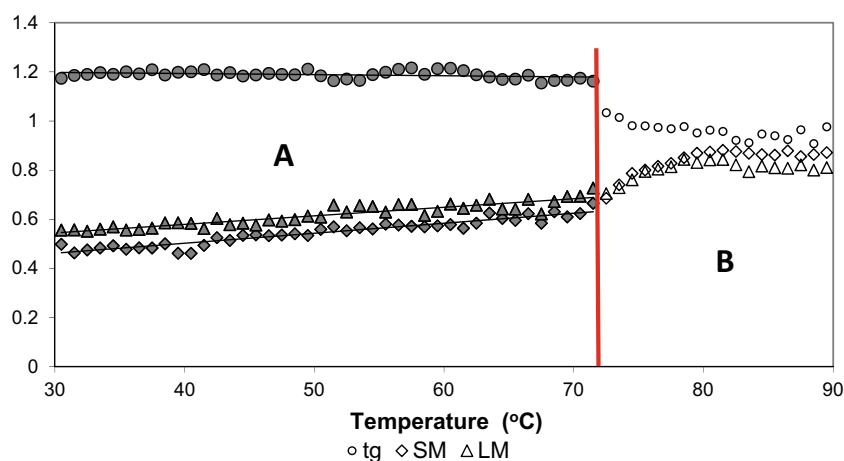

Fig. 4 Ratio of initial DMA value measured at the same stage of the temperature scan in pulsed and initial state. *SM* denotes ratio of storage (real part) module, *LM* ratio of loss (imaginary part) module, and *tg* ratio of loss tangents (ratio of loss and storage module). The *thick line* at temperature 71.5 °C approximates the border between the basic parts of

the temperature scale: A and B. In part A, the temperature plots are linearly approximated: $SM = 0.0041T + 0.3395, R^2 = 0.903$, $LM = 0.0035T + 0.4403, R^2 = 0.843$, $tg = -0.0005T + 1.211, R^2 = 0.123$, where T is temperature (°C)
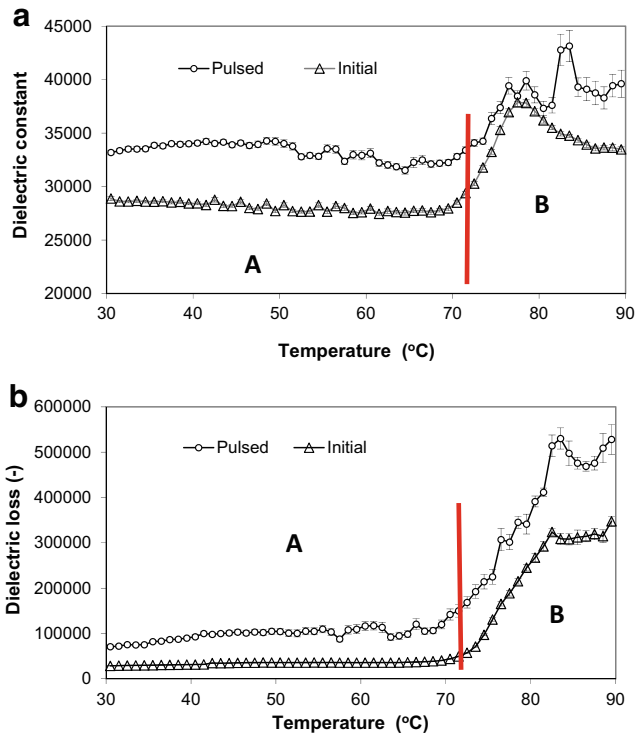
Fig. 5 The basic DETA data: temperature plots of the dielectric constant (Fig. 5a) and dielectric loss (Fig. 5b). The *bars* denote standard errors, *Initial* denotes results on the specimens without electric pulses, and *Pulsed* denotes the results on the pulsed specimens. The *thick line* at temperature 71.5 °C approximates the border between the basic parts A and B of the temperature scale

increase (B2) was observed, too. More variability was observed at ratios of DL (dielectric loss) and tg (loss tangent); this variation was observed even at temperatures in part A. The smoothing mechanism had to be used in this case to obtain more clear data. Even if the ratios of DL and tg approximately increased in the whole part A (up to approximately 71 °C), some smaller peaks were also observed inside of this: at 41.5, 47.5, and 61.5 °C. These changes were much less than the main change obtained on the border to the range B,
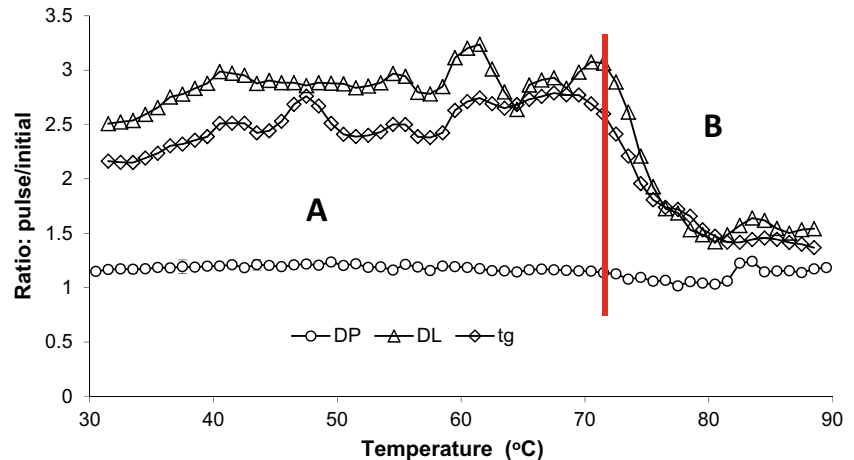
approximately at 71 °C. In this place, there was observed starting of a fall more than about 50 % to values little more than 1, so that the data for the pulsed specimens were approximately the same as the corresponding data for the initial specimens (see Fig. 5).

We recalculated also the impedance values (Kindl 2014) from the permittivity data and the calculated ratios of the corresponding values in the groups prepared with and without pulses. The obtained results are plotted in Fig. 7. In this plot, there is also a clearly visible border between the low temperature (A) and the higher temperature range (B) of the temperature scale, approximately at 71.5 °C where the total minima of the plots are located. In the lower part of the temperature scale (A), the values of the ratios approximately decreased, whereas at higher temperatures, the plots were of increased character at least in some fraction of the temperature scale (the range B). Some additional characteristic points can be found at the plots in Fig. 7 in both temperature parts. The values of both ratios in Fig. 7 are lower than 1, so that both impedance components in pulsed carrot were lower than the impedance of the initial carrot tissue. The initial values of the ratios at 30 °C were about 0.65 (real part) and 0.30 (imaginary part) in good agreement with data in Fig. 2 at a field intensity of 600 V/cm and time of 120 s after pulsing. Total minima of the plots at 71.5 °C corresponded to the values 0.4 (real part) and 0.16 (imaginary part). The maximal values at 80 °C were still less than 1: 0.72 for the real part of impedance and 0.52 for its imaginary part.

We try to estimate the disintegration parameter Z from Eq. (1) for the whole tests; it could be expressed using the impedances as follows:

$$Z = \frac{\frac{z_u}{z}-1}{\frac{z_u}{z_d}-1} \qquad (3)$$

where the carrot impedances are used: z_u for the initial state before the tests, z for the evaluated state, and z_d for the

Fig. 6 Ratio of the data (see Fig. 5) obtained in the tests on the pulsed specimens and the initial ones plotted against temperature. For description, the following symbols are used: *DP* dielectric constant, *DL* dielectric loss, and *tg* ratio DL/DP (loss tangent). The data were smoothed by the mean values of the three adjacent values. The *thick line* at temperature 71.5 °C approximates the border between the basic parts A and B of the temperature scale
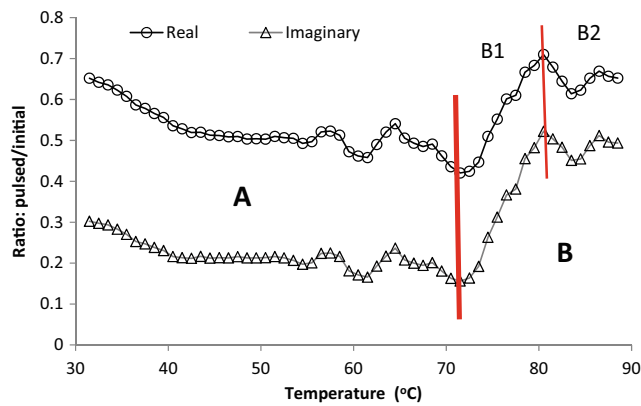
Fig. 7 Ratio of the impedance data (calculated from the permittivity data in Fig. 5) obtained in the tests on the pulsed specimens and the initial ones plotted against temperature. Real component of the impedance is denoted as *real* and the imaginary component is denoted similarly. The data were smoothed by the mean values of the three adjacent values. The *thick line* at temperature 71.5 °C approximates the border between the basic parts A and B of the temperature scale. Scale B is divided into two subparts, B1 and B2

destructed state. The parameter z_d was not determined in our test, so that we will use the minimal observed value as an estimation of it. Moreover, z measured at the actual temperature is put into Eq. (3) comparing it with the initial value z_u measured at room temperature. The resulting values are in Fig. 8. Below approximately 71.5 °C, i.e. in temperature range A, the parameter Z is relatively constant and below 0.01 for specimens that were not electrically pulsed and in the range 0.08–0.17 for specimens previously pulsed in electric field. In temperature range B, the parameter Z increased rapidly with increasing temperature reaching more stable values at temperatures above 82 °C (close to 0.5 for specimens without pulsing and above 0.85 for the pulsed ones).

Common Indications of DMA and DETA

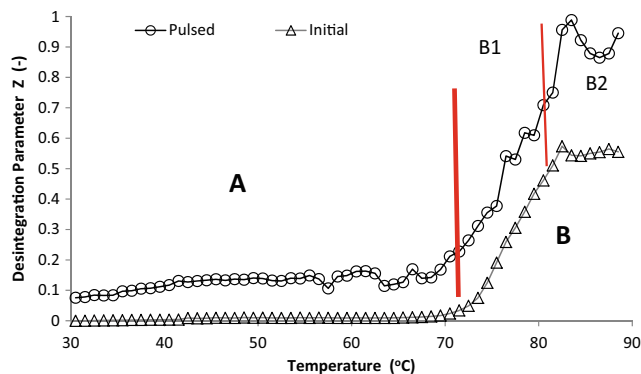We use the defined temperature ranges, A and B. Range B was divided onto two parts: B1 (at temperatures between

Fig. 8 Parameter Z from Eq. (1) calculated under Eq. (3). The impedance of disintegrated tissue was estimated as the minimal observed value. *System of borders* is the same as in Fig. 7

approximately 71.5 and approximately 80 °C) and B2 (at temperatures higher than approximately 80 °C)—see Fig. 7. The border between ranges A and B is denoted by the thick lines in Figs. 4, 5, 6, and 7. Part B1 is a part of the temperature scale, where the differences caused by pulsing are reduced (Figs. 4, 6, 7, and 8). The differences between values measured in the pulsed specimens and the initial ones were minimized in part B2 where for mean values of parameters in Fig. 4 were obtained 0.87, 0.82, and 0.94 for SM, LM, and LM/SM, respectively. Coefficient of variation was less than 2.5 % in all cases. Similarly for the electrical measurements, the values 0.66 and 0.44 were observed for ratios of real and imaginary impedance parts, respectively.

The trends of changes and the range structure given by DETA and DMA are the same. The range A conserves the changes made by the electric pulses prior the DMA test and/or the DETA test. Part B1 can be classified as the temperature part in which new big changes at least partly reduce the changes caused by the previous pulse procedures. Most observed results can be explained by increasing permeability of the cellular membranes that is followed by decreasing intracellular pressure (Blahovec and Lahodová, 2011). The permeability of cellular membranes was increased either by electric pulsing or standardly by heating the tissue in temperature range B, mainly in part B1. In part B2, the process of increasing the membrane permeability stagnated, probably due to exhausting the potential sources followed by some alternative mechanisms. Trying to keep some pulse effects in carrot and/or in the other vegetables, the critical temperature between the ranges A and B should not be exceeded.

Result Applications

The superposition of short electric pulses prior to the heating and the heating in part A is a form of a *low-temperature cooking* of carrot and similar vegetables. The electric pulses caused an initial long time decrease of the tissue texture (in the form of an elastic module that is represented by a 50 % decrease in 2 min after pulsing), and the further decrease was caused by the following heating (Peng et al., 2014, De Roeck et al., 2010, Kidmose and Martens, 1999). Some part of a pulsed tissue is "opened" by the pulses. The level of damage should be higher than parameter Z (Fig. 8), i.e. ≈10 %. This value is under our view underestimated because the parameter z_d and also z was not determined correctly and they were estimated by a value that was obtained in different conditions at high temperatures. A more realistic value can be obtained from ratio i of real part of the electric impedance in Fig. 7. The degree of the damaged cellular membranes d in the pulsed tissue is then given as $d = 1 - i$, and this is in our case ≈35 %. Similarly as the texture, also cell opening has a long time character and it is stable in the whole temperature range A (Figs. 5, 6, 7, and 8). The heating that could be termed as a low-temperature blanching (Lemmens et al., 2009) forms a

part of the procedure necessary for stabilization of the product (Lemmens et al., 2009, Leong and Oey, 2014). The combination of short electric pulses with the low-temperature heating should be energetically more efficient than the classical long time cooking at high temperatures. The optimal combinations of different pulse regimes and the low-temperature cooking should be analysed in further research.

Conclusions

The texture of carrot decreases after electric pulsing at room temperature; in our case, one 10 ms AC pulse (frequency, 10 kHz) with a field intensity of 600 V/cm caused a 50 % decrease of elastic module. This level of applied pulses causes a decrease of the real component of electric impedance about 35 % indicating strong damage of cellular membranes. The changes caused by pulsing are stable during the heating scan in temperature range A up to about 70 °C. Above this temperature in range B, both mechanical parameters (DMA) and electrical parameters (DETA) indicate further destruction of the cellular structure.

Comparing the effects of electric pulsing in the temperature range A and heating in the temperature range B, we can see nontrivial similarity between them. We can term both procedures as cooking of carrot with the first step in the temperature range A (electrical pulsing) and the second step in range B (traditional heating). Both steps can have a lot of different modifications that could be studied separately.

References

Ando, Y., Mizutani, K., & Wakatsuki, N. (2014). Electrical impedance analysis of potato tissues during drying. *Journal of Food Engineering, 121*, 24–31.

Blahovec, J., & Lahodová, M. (2011). DMA peaks in potato cork tissue of different mealiness. *Journal of Food Engineering, 103*, 273–278.

Blahovec, J., & Lahodová, M. (2012a). Changes in carrot (*Daucus carota*) parenchyma at higher temperatures detected in vivo by dynamic mechanical (thermal) analysis. *Biorheology, 49*, 289–298.

Blahovec, J., & Lahodová, M. (2012b). DMA thermal analysis of different parts of potato tubers. *Food Chemistry, 133*, 1101–1106.

Blahovec, J., Lahodová, M., & Zámečník, J. (2012). Potato DMA analysis in area of starch gelatinization. *Food Bioprocess Technology, 5*, 929–938.

De Roeck, A., Mols, J., Duvetter, T., Van Loey, A., & Hendrickx, M. (2010). Carrot texture degradation kinetics and pectin changes during thermal versus high-pressure/high-temperature processing: a comparative study. *Food Chemistry, 120*, 1104–1112.

De Vito, F., Ferrari, G., Lebovka, N. I., Shynkaryk, N. V., & Vorobiev, E. (2008). Pulse duration and efficiency of soft cellular tissue disintegration by pulsed electric fields. *Food and Bioprocess Technology, 1*, 307–313.

Garret, R. H., & Grisham, C. M. (2010). *Biochemistry* (4th ed.). Boston: Brooks/Cole.

Georget, D. M. R., Smith, A. C., & Waldron, K. W. (2002). Dynamic mechanical thermal analysis of cell wall polysaccharides extracted from lyophilised carrot *Daucus carota. Carbohydrate Polymers, 48*, 277–286.

Gómez, F., Toledo, R. T., Wadsö, L., Gekas, V., & Sjöholm, I. (2004). Isothermal calorimetry approach to evaluate tissue damage in carrot slices upon thermal processing. *Journal of Food Engineering, 65*, 165–173.

Gómez Galindo, F., Wadsö, L., Vicente, A., & Dejmek, P. (2008). Exploring metabolic responses of potato tissue induced by electric pulses. *Food biophysics, 3*, 352–360.

Haines, P. J. (2002). *Principles of thermal analysis and calorimetry*. Cambridge: The Royal Society of Chemistry.

Hiranvarachat, B., Devahastin, S., & Chiewchan, N. (2011). Effects of acid pretreatments on some physicochemical properties of carrot undergoing hot air drying. *Food and bioproducts processing, 89*, 116–127.

Hoaglin, D., Mosteller, F., & Tukey, J. (1983). *Understanding robust and exploratory data analysis*. New York: Wiley.

Kidmose, U., & Martens, H. J. (1999). Changes in texture, microstructure and nutritional quality of carrot slices during blanching and freezing. *Journal of the Science of Food and Agriculture, 79*, 1747–1753.

Kindl, M. (2014). *Thermal analysis applied to quality evaluation of pulses and row crops (in Czech)*. Ph.D. Thesis. Czech University of Life Sciences, Prague.

Kittel, C. (2005). *Introduction to solid state physics*. New York: Wiley.

Lebovka, N. I., Bazhal, M. I., & Vorobiev, E. (2002). Estimation of characteristic damage time of food materials in pulsed-electric fields. *Journal of Food Engineering, 54*, 337–346.

Lemmens, L., Tibäck, E., Svelander, C., Smout, C., Ahrné, L., Langton, M., Alminger, M., Van Loey, A., & Hendrickx, M. (2009). Thermal pretreatments of carrot pieces using different heating techniques: effect on quality related aspects. *Innovative Food Science and Emerging Technologies, 10*, 522–529.

Leong, S. Y., & Oey, I. (2014). Effect of pulsed electric field treatment on enzyme kinetics and thermostability of endogenous ascorbic acid oxidase in carrots (*Daucus carota* cv. Nantes). *Food Chemistry, 146*, 538–547.

Lešková, E., Kubíková, J., Kováčiková, E., Košická, M., Porubská, J., & Holčíkova, K. (2006). Vitamin losses: retention during heat treatment and continual changes expressed by mathematical models. *Journal of Food Composition and Analysis, 19*, 252–276.

Park, S. H., Balasubramaniam, V. M., & Sastry, S. K. (2013). Estimating pressure induced changes in vegetable tissue using in situ electrical conductivity measurement and instrumental analysis. *Journal of Food Engineering, 114*, 47–56.

Peng, J., Tang, J., Barrett, D. M., Sablani, S. S., & Powers, J. R. (2014). Kinetics of carrot texture degradation under pasteurization conditions. *Journal of Food Engineering, 122*, 84–91.

Šmejkal, E., Yurov, A., & Blahovec, J. (2011). Device for study of electric pulse after-effect in vegetable tissue. *Jemná mechanika a optika, 56*(5), 153–155.

Tsong, T. Y., & Su, Z.–. D. (1999). Biological effects of electric shock and heat denaturation and oxidation of molecules, membranes, and cellular functions. *Annals of New York. Academy of Sciences, 888*, 211–232.

Vollmer, M. (2004). Physics of the microwave oven. *Food Physics, 39*, 74–81.

Vorobiev, E., Lebovka, N. (2008). Pulsed-electric-fields-induced effects in plant tissues: fundamental aspects and perspectives of applications. In: *Electrotechnologies for extraction from food plants and biomaterials*, E. Vorobiev and N. Lebovka (eds.), doi: 10.1007/978-0-387-79374-0 2, C Springer Science+Business Media, p. 39-81.

Vorobiev, E., & Lebovka, N. (2010). Enhanced extraction from solid foods and biosuspensions by pulsed electrical energy. *Food Engineering Review, 2*, 95–108.

Xu, C., & Li, Y. (2014). Development of carrot parenchyma softening during heating detected in vivo by dynamic mechanical analysis. *Food Control, 44*, 214–219.